MEASURING THE ANGLE OF A ROTATING LINK THROUGH COMPLIANT DRIVING TENDONS

Mark L. Guckert[1] *and Michael D. Naish*[1,2]

[1]Department of Mechanical & Materials Engineering
[2]Department of Electrical & Computer Engineering
The University of Western Ontario
London, Ontario, Canada N6A 5B9

ABSTRACT

Measuring the position of a tendon-driven rotating link, based on the state of the tendons at the proximal end is challenging. Specifically, tendon elasticity and Coulomb friction can cause significant nonlinearities in the relationship between the motion at the proximal end of the tendon and the motion of the link. An extended Kalman filter (EKF) is proposed as a potential method to refine estimates of link position based on proximal measurements. A model link and tendon system is built to demonstrate the impact of these effects on measurement. Sensors are incorporated to allow direct measurement of the link position in addition to the motion of the tendons at their origins. A dynamic model is developed for the resulting system and used in conjunction with an EKF to generate improved estimates of the link's motion based on proximal measurements alone.

Index Terms— tendon actuator, compliant tendons, proximal measurement, rotating link, extended Kalman filter

1. INTRODUCTION

The idea of driving a manipulator via cable-tendons has been explored in many branches of manipulator design. It has been incorporated into serial manipulators, parallel manipulators, continuum, and high degree of freedom (DOF) manipulators. Tendons have been used extensively because they present several advantages, predominantly that driving a manipulator through tendons allows the actuators to be situated remotely on the manipulator base, allowing the manipulator to be made more lightweight and compact. This removal of manipulator bulk allows the manipulator to achieve greater accelerations, lift heavier payloads, and operate in spaces that would otherwise not be possible. The tendon transmission system does, however, present additional complications to the mechanical design and control of the manipulator, such as extra mechanical components, friction, tendon compliance, and increased kinematic complexity. It has been demonstrated that these complications can be compensated for as in [1] and [2], allowing systems with remarkable payload and dexterity characteristics to be created such as the CT arm [3] or the SEGESTA parallel manipulator [4].

To ensure accurate position control of a manipulator, the state of each joint must be known with relative precision. Often sensors are incorporated directly into each joint, adding to the volume and mass of the manipulator. In demanding situations, where sensors at each joint will significantly increase the weight and size of a manipulator, it would be advantageous to locate sensors proximally and sense the position of joints through tendons. This approach has been explored with serial-type manipulators, as in the CT arm [3] and several continuum manipulators [5], but these do not employ any compensation for tendon dynamics. Although [6] presents a method of compensating for tendon-sheath interactions along a single tendon, little has been done to take advantage of feedback from an antagonistic pair of actuating tendons coupled with knowledge of a tendon model.

Most conventional tendon driven manipulators use sufficiently stiff tendons, typically steel cables, so that the effects of tendon stretch may be neglected. This, however, requires tendons which are bulkier and more difficult to route through a manipulator than more flexible ones. Also, in manipulators designed for physical interaction with humans, a degree of passive compliance is often required in order to limit forces which may potentially be applied to a person. In such situations, where tendon elasticity is required, only conventional measurements of joint angles will provide an accurate measure of manipulator position. In this paper, a method of more accurately estimating the position of a rotating link through highly compliant tendons, using an extended Kalman filter (EKF) is proposed.

This paper proposes to explore the effects of high tendon compliance and Coulomb friction on the monitoring of a single rotating link through tendons and examine a potential approach through which the detrimental influence of these system characteristics on measurement can be reduced. The influence of these system properties are compared to those predicted by a dynamic model of the system, allowing for evaluation of the model's accuracy and potential limitations. The developed model is then used as part of an EKF to test the effectiveness of exploiting knowledge of the system to compensate for the effects of dry friction and tendon elasticity in monitoring the joint angle of a single link through tendons.

2. METHOD

2.1. Experimental Setup

In the experimental apparatus, the rotating link consists of a simple disk made of 3 mm thick fiberboard weighing 84 g. This disk is fixed to a base by a $\frac{1}{4}$" Allen bolt, passing through the disk centre, with washers separating the disk from the bolt head and base, allowing the link to rotate freely. The link is driven by tendons with insertions set opposite each other 9.5 mm from the disk centre. Multistrand nylon thread, 0.2 mm in diameter, is used to make the tendons themselves, with the tendon stiffness being increased by adding parallel threads. The tendon stiffness reported is based upon measurements

This research was supported in part by the Natural Sciences and Engineering Research Council (NSERC) of Canada under grant 312383-05.

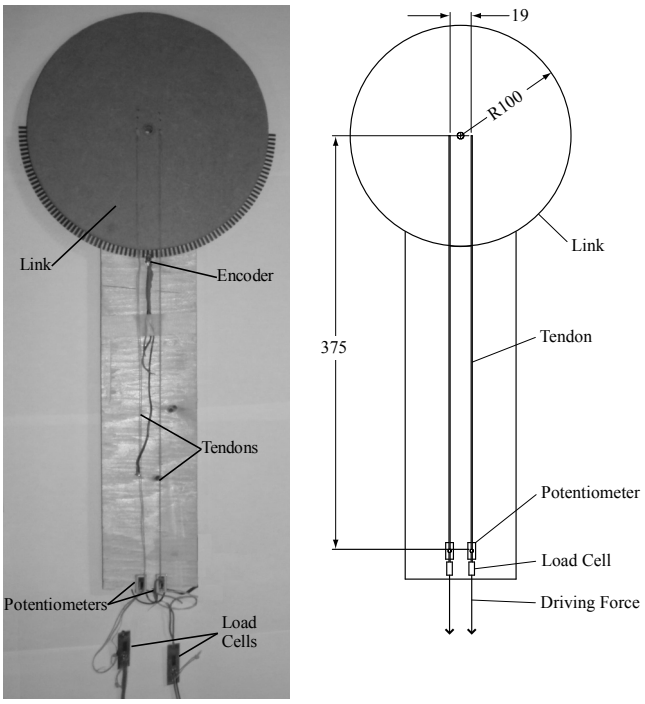

Fig. 1. Experimental apparatus (dimensions in mm).

of tendon deformation due to applied loads between 6 and 10 N. The tendon origins consist of two linear potentiometers (Panasonic EVA-W7NR04B34) positioned 375 mm from the link axis. These are used to sense the proximal displacement of the tendon. The potentiometers present a linearity error of $\pm 1\%$ of the full scale and a random error of ± 0.01 mm in their measurements. Two load cells measure the driving forces applied to the system, made from $30\times 9\times 0.8$ mm aluminum and a strain gauge (Showa N11-FA-5-120-11). Measurements from these load cells are quite noisy, on the order of ± 0.6 N. Driving forces are applied by attaching weights to the bottoms of the load cells. The experimental apparatus is illustrated in Fig. 1.

The angular position of the link is monitored independently using an optical encoder (Panasonic CNA1302K) with a resolution of 1°. This provides a baseline measurement against which all other position measurements can be compared. The output of the five sensors used in this apparatus are all recorded using a PC equipped with a National Instruments PCI-6221 data acquisition (DAQ) board, at a sampling rate of 100 Hz.

2.2. Dynamic Model

The system presents a number of inherent nonlinearities in its dynamics. Aside from the effects of dry friction, the relationship between link and potentiometer motion is entirely nonlinear. The counterclockwise motion of the link θ, the left potentiometer x_1, and the right potentiometer x_2, are modeled as shown in (1), (2), and (3) respectively, with both positive x_n directions considered to be away from the link. The finite range of motion available to the potentiometers must also be taken into account in an accurate dynamic model of the system. This is done by including the function $F_{\text{stop}}(x_n)$, which applies a large elastic response and viscous damping when the potentiometers meet the end of their range of motion. This response is defined in (14), where $x_{n_{\text{stop}}L}$ and $x_{n_{\text{stop}}H}$ represent the minimum and maximum positions to which the tendon's proximal end can move, respectively. A list of all constant model parameters, their descriptions, and values used is included in Table 1.

Table 1. Dynamic model parameters.

Variable	Description	Value	Units
J	link moment of inertia	4.239×10^{-4}	kg·m^2
m_1	mass of potentiometer 1	1×10^{-3}	kg
m_2	mass of potentiometer 2	1×10^{-3}	kg
k	spring constant of tendons	806	N/m
r	length from link axis to tendon	9.53×10^{-3}	m
L_i	initial, unloaded tendon length	0.375	m
B_{v_θ}	viscous damping on link	8×10^{-3}	N·m·s
r_{axle}	radius of link axle	3.18×10^{-3}	m
μ_θ	coefficient of friction at link axle	0.5	none
T_0	dry friction prior to tensions	4.9	N
B_v	potentiometer viscous damping	0.01	kg/s
μ	potentiometer coefficient of friction	2×10^{-3}	none
B_{stop}	viscous damping at potentiometer end of range of motion	3.0	kg/s
k_{stop}	spring constant at potentiometer end of range of motion	1×10^5	N/m

$$J\ddot{\theta} + B_\theta(\dot{\theta}, T_1, T_2) = \tau_1 - \tau_2 \tag{1}$$

$$m_1\ddot{x}_1 + B(\dot{x}_1, T_1) + T_1\cos\phi_1 = U_1 - F_{\text{stop}}(x_1) \tag{2}$$

$$m_2\ddot{x}_2 + B(\dot{x}_2, T_2) + T_2\cos\phi_2 = U_2 - F_{\text{stop}}(x_2) \tag{3}$$

In the equations above, T_1 is the tension in the left tendon, T_2 is the tension in the right tendon, $B_\theta(\dot{\theta})$ is the friction torque applied to the link, $B(x_n)$ is the friction force applied to the potentiometers, and U_1 and U_2 are the driving forces applied to the left and right potentiometers respectively. The tensions T_1 and T_2 in the tendons are calculated as a function of the potentiometer and link positions and generate torques τ_1 and τ_2 on the link, respectively. These tensions and torques are found through (8), (9), (10), and (11). The variables L_1 and L_2 represent the changing distance between the tendon origin and insertion and the variables. ϕ_1 and ϕ_2 are the angles between the current tendon path and the tendon path before link rotation.

$$L_1 = \sqrt{r^2(1-\cos\theta)^2 + (L_i + x_1 - x_{1i} - r\sin\theta)^2} \tag{4}$$

$$L_2 = \sqrt{r^2(1-\cos\theta)^2 + (L_i + x_2 - x_{2i} - r\sin\theta)^2} \tag{5}$$

$$\phi_1 = \arctan\big(r(1-\cos\theta)/(L_i + x_1 - x_{1i})\big) \tag{6}$$

$$\phi_2 = \arctan\big(r(1-\cos\theta)/(L_i + x_2 - x_{2i})\big) \tag{7}$$

$$T_1 = k(L_1 - L_i + x_{1i}) \tag{8}$$

$$T_2 = k(L_2 - L_i + x_{2i}) \tag{9}$$

$$\tau_1 = T_1 r\left(\cos\theta\cos\phi_1 - \sin\theta\sin\phi_1\right) \tag{10}$$

$$\tau_2 = T_2 r\left(\cos\theta\cos\phi_2 - \sin\theta\sin\phi_2\right) \tag{11}$$

The variables x_{1i} and x_{2i} represent the length of tendon allowed to slip past the attachment point on the potentiometers so that their full range of motion can be utilized. Functions B_θ and B are defined as (12) and (13) respectively, where T_0 is a value assigned to represent the dry friction contribution from the weight of the link on the axle and the clamping force applied to the link by its axle.

$$B_\theta = \begin{cases} \tau_1 - \tau_2 & \text{if } |\tau_1 - \tau_2| < \mu_\theta r_{\text{axle}}(T_1 + T_2 + T_0) \text{ and } \dot{\theta} = 0 \\ \mu_\theta r_{\text{axle}}(T_1 + T_2 + T_0) \operatorname{sgn} \dot{\theta} + B_{v_\theta}\dot{\theta} & \text{otherwise} \end{cases} \tag{12}$$

$$B = \begin{cases} U_n - T_n \cos\phi_n - F_{\text{stop}} \\ \quad \text{if } \left|U_n - T_n \cos\phi_n - F_{\text{stop}}\right| < \mu T_n \text{ and } \dot{x}_n = 0 \\ \mu T_n + B_v \dot{x}_n \quad \text{otherwise} \end{cases} \tag{13}$$

$$F_{\text{stop}} = \begin{cases} k_{\text{stop}}(x_n - x_{n_{\text{stop}H}}) + B_{\text{stop}}\dot{x}_n & \text{if } x_n > x_{n_{\text{stop}H}} \\ k_{\text{stop}}(x_n - x_{n_{\text{stop}L}}) + B_{\text{stop}}\dot{x}_n & \text{if } x_n > x_{n_{\text{stop}L}} \\ 0 & \text{otherwise} \end{cases} \tag{14}$$

These dynamic equations were used to simulate the system in MATLAB using the `ode23` function. The EKF was also implemented as a MATLAB function, used solely for offline processing of test measurements. For this filter, the process (Q) and measurement (R) noise covariance matrices were used as tuning parameters and, for the sake of simplicity, assumed to be time-invariant, scalar products of the identity matrix, as detailed information regarding these errors was not readily available [7]. Each data set was first filtered with the estimate covariance (P) initially set to 1. The final P from this filtration was then used as a more suitable initial P to refilter the run.

2.3. Testing

Testing of this measurement system was conducted by first applying a series of known, equal driving forces to the tendon origins with weights. The link was then forced through a simple sequence of motions: first to the furthest clockwise position possible, without driving the potentiometers to the limits of their range of motion, then to the furthest counterclockwise position allowed. This sequence of tests was repeated with a second set of tendons with a stiffness twice that of the first. These tests were conducted to observe the effects of tendon stiffness and Coulomb friction on measurements by comparing the optical encoder position measurements with those estimated from the proximal tendon displacement measurements, assuming tendon stretch to be zero. The results of this test would be analogous to a manipulator having an external force applied to its end effector, and attempting to estimate the resulting motion of the end effector based on tendon motion at the proximal end, without any compensation for tendon stretch or friction losses.

A second series of tests were conducted, with the stiffer tendons, by applying two unequal loads to the tendons and allowing the link to rotate freely. Throughout these tests, the DAQ board was used to measure the tendon position at the origins, the driving forces applied to the system, and the link displacement as measured by the encoder.

The EKF was then used to estimate the link position from the proximal tendon measurements collected in the second series of tests. The link position estimate generated by the filter could then be compared to the displacement measurement from the optical encoder, as well as the link position as estimated from the proximal tendon displacements, assuming tendon elasticity to be negligible.

3. RESULTS AND DISCUSSION

3.1. Without Compensation for Tendon Dynamics

From the initial tests, the detrimental effects of friction and tendon elasticity can be readily seen, Fig. 2. Here the "Encoder" data represents the link position as reported by the encoder, and "Pot 1" and "Pot 2" are the link position as estimated from the potentiometer readings with the tendon assumed to be inelastic. In these tests, constant, equal driving forces were applied to the proximal end of the tendons while the link was moved by an unmeasured external force.

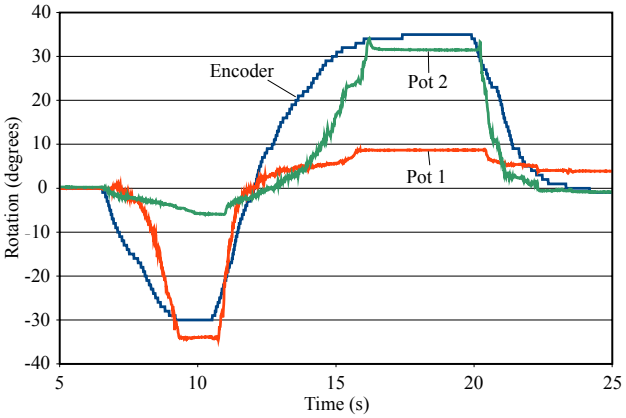

Fig. 2. Link position with 2 N driving load. k = 403 N/m.

Fig. 2 demonstrates that the effects of system dynamics mask any sensor errors in estimating link motion from the tendon displacements. The linearity error from the potentiometers contributes less than $\pm 0.6^\circ$ error, in the ideal case involving inelastic tendons, and far more error is observed. Also, the tendon whose tension opposes the motion of the link presents a more accurate representation of the motion at the distal end of the link. Such a result is anticipated, as the tendon opposing motion will face increasing tension as frictional forces act against tendon motion, while the tendon assisting motion will only lose tension as frictional forces oppose its motion, providing less correlation between link and tendon motion. It was noted that, error was reduced by doubling the tendon stiffness; however, the system responses were similar and error remained significant.

It can be clearly seen from these results that estimates of link rotation (in any system with appreciable tendon stretch and Coulomb friction) made from the proximal end of tendons may not represent link motion at all, if tendon dynamics are not compensated for.

3.2. Compensating for Tendon Dynamics using EKF

Initial trials with the EKF provide promising results, as can be seen in Fig. 3. The filtered link position signal (labeled "Filtered") is far closer to the actual link position than that simply estimated from the tendon displacements. In this test, the link was driven by forces of 2 N and 6 N applied at the tendon origins. For all filtered results shown here, the EKF had been tuned using 0.001 for both Q and R. This value was selected as it seemed to provide a balance between the simulated and measured position data, favouring the measured values of the tendon displacements more heavily in most trials.

Fig. 4 shows results from subsequent runs repeated with higher tendon forces. It is clear from these results that higher tendon forces magnify the effects of tendon dynamics and their influence on position measurements as seen from the proximal end. Nonetheless, as demonstrated in Fig. 5, filtered proximal measurements can provide an improved estimate of distal link rotation, as compared to estimates made without any compensation for the tendon dynamics. Clearly the effects of Coulomb friction are being underestimated in simulation, as the applied tension increases. From Fig. 3 it may be observed that the motion of the system under lower forces is closely

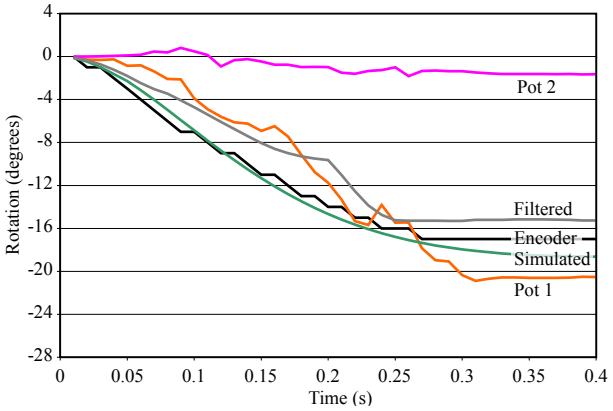

Fig. 3. Various measures of link position from a single run. Driving forces are U_1 = 2 N and U_2 = 6 N; k = 806 N/m.

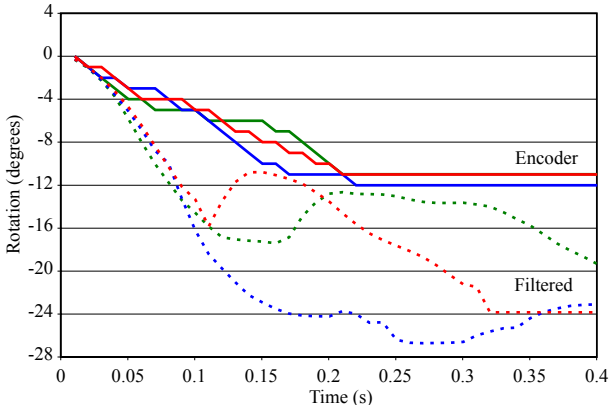

Fig. 4. Encoder and filtered positions over repeated runs. Driving forces are U_1 = 1 N and U_2 = 8 N; k = 806 N/m.

mimicked by the simulation. However, as the tension increases, as in Fig. 5, the link motion is overestimated. This additional rotation of the simulated link is likely due to increasing friction losses with increased tension not being properly reflected in the dynamic model.

Finally, it was noted through direct observation of the EKF during filtering of several runs that, since the driving load measurements were relatively noisy (approximately $\pm$0.6 N), the EKF largely ignores this data, instead favouring the direct measurements of tendon displacements. This effectively eliminates the benefit of measuring the driving forces to better estimate the link position.

4. CONCLUSIONS

In this paper, the limitations inherent to sensing the position of a rotating link through compliant driving tendons has been presented in brief. The effects of tendon stretch and Coulomb friction can combine to make estimates of link motion based on tendon displacement at the proximal end entirely inaccurate. The impact of these effects can be so detrimental, in cases of appreciable tendon elasticity, that accurate position control of a link would be entirely impossible without some form of compensation for tendon dynamics.

It has been demonstrated that by using a sufficiently representative dynamic model of the system in question, in concert with an EKF, a more refined estimate of link position could be made based on

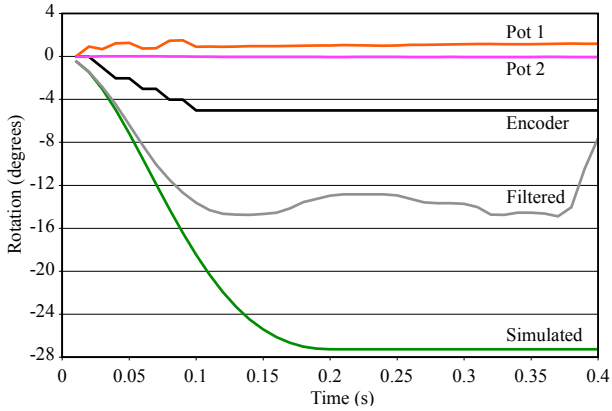

Fig. 5. Various measures of link position from a single run. Driving forces are U_1 = 1 N and U_2 = 10 N; k = 806 N/m.

the state of the tendons at the proximal end than could be made if the tendon dynamics were ignored. Such an approach could easily find application in the design of manipulators requiring accurate position control which, by allowing sensors to be placed at the proximal end of tendons, would allow manipulators to be made both lighter and smaller. Similarly, this approach could also allow manipulator designs with joint sensors already located proximally to improve their accuracy or to employ more flexible tendons which would, in turn, ease the routing of tendons through the manipulator. These potential improvements could lead to new applications in which more accurate compliant manipulators could be used in interaction with humans.

The use of more accurate load cells could serve to improve the measurement system presented here, by allowing the EKF to rely more heavily on their measurements and generate more accurate estimates of link position. The system's dynamic model could also be improved by incorporating a more accurate depiction of the system's frictional losses, which would, consequently, improve the filter.

5. REFERENCES

[1] S. C. Jabobsen, H. Lo, E. K. Iversen, and C. C. Davis, "Control strategies for tendon-driven manipulators," *IEEE Control Syst. Mag.*, vol. 10, pp. 23–28, Feb. 1990.

[2] H. Kobayashi and R. Ozawa, "Adaptive neural network control of tendon-driven mechanisms with elastic tendons," *Automatica*, vol. 39, pp. 1509–1519, Sept. 2003.

[3] S. Ma, S. Hirose, and H. Yoshinada, "Design and experiments for a coupled tendon-driven manipulator," *IEEE Control Syst. Mag.*, vol. 13, pp. 30–36, Feb. 1993.

[4] F. Shiqing, D. Franitza, M. Torlo, F. Bekes, and M. Hiller, "Motion control of a tendon-based parallel manipulator using optimal tension distribution," *IEEE/ASME Trans. Mechatron.*, vol. 9, pp. 561–568, Sept. 2004.

[5] B. A. Jones and I. D. Walker, "Kinematics of multisection continuum robots," *IEEE Trans. Rel.*, vol. 22, pp. 43–55, Feb. 2006.

[6] G. Palli and C. Melchiorri, "Model and control of tendon-sheath transmission systems," in *Proc. IEEE Int. Conf. on Robotics and Automation*, Orlando, Florida, May 15–19, 2006, pp. 988–993.

[7] I. R. Peterson and A. V. Savkin, *Robust Kalman Filtering for Signals and Systems with Large Uncertainties*. New York, NY: Birkh auser Boston, 1999.